Revealing Interfaces and Nanostructure: The Application of Atom Probe Tomography to Nickel Based Superalloys

Dr. Chantal Sudbrack, NASA Glenn Research Center, chantal.k.sudbrack@nasa.gov

1. Background in nickel-based superalloys
2. Background in atom-probe tomography
3. Decomposition behavior of model Ni-Al-Cr alloy when aged at 600 °C

Acknowledgements: Prof. David Seidman, Kevin E. Yoon , Zugang Mao (Northwestern); Ronald Noebe (NASA GRC); Georges Martin (Comm. à l'Energie Atomique); Northwestern University Center for Atom Probe Tomography (NUCAPT)

Poster: The effect of prior exposures on the notched fatigue behavior of disk superalloy ME3

Co-authors: Susan L Draper[1], Timothy T Gorman[2], Jack Telesman[1], Timothy P Gabb[1], David R Hull[1], Daniel E Perea[3] and Daniel K Schreiber[3] : 1. NASA Glenn 2. NASA USRP 3. PNNL

May 15, 2013

Ni-Based Superalloys

Due to an unusual combination of properties, Ni-based superalloys are used in many applications which require structural integrity at elevated temperatures

Precipitate strengthened

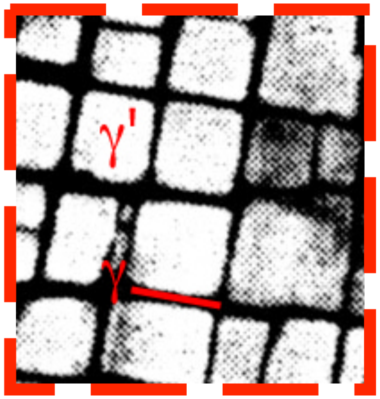

Mechanical properties

- Capable of bearing loads at T/T_M = ~0.85-0.9 ($T_{M(Ni)}$ = 1453˚C) without significant deformation
  - – γ' strengthening (precipitatestrengthening)
  - – Solid solution strengthening in the γ-matrix
- Damage Tolerance (Ductility and Toughness)

Requirements:

- Resistance to Environmental Degradation
  - – Hot corrosion and oxidation

Turbine Jet Engine

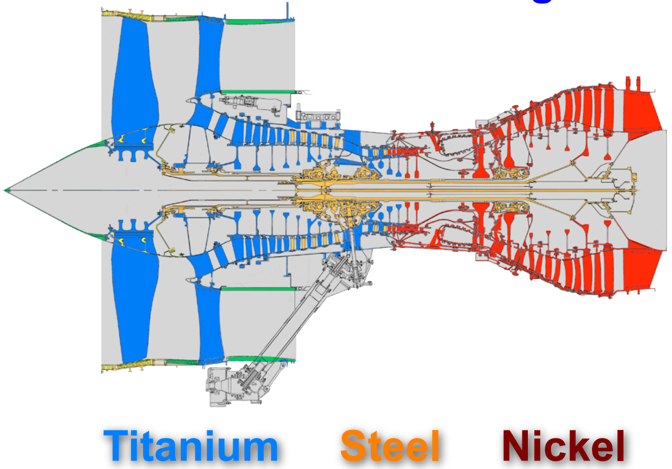

- **Single Crystal Ni-Based Superalloys**
  - Engineered for Extreme Temperature Capability - Creep, Thermal Fatigue and Environmental Protection
  - Anisotropic Properties
  - Turbine Blade and Nozzle Applications *NASA GRC*

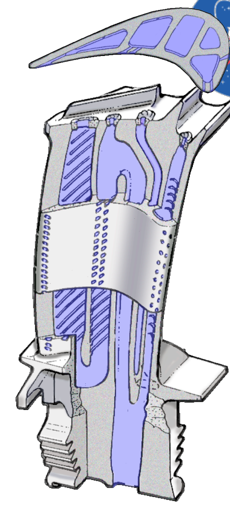

- **Polycrystalline Ni-Based Superalloys**
  - Intermediate Temperature Capability – Fatigue, Tensile, Crack Growth and Environmental Resistance
  - Isotropic Properties
  - Turbine Disk Applications *NASA GRC*

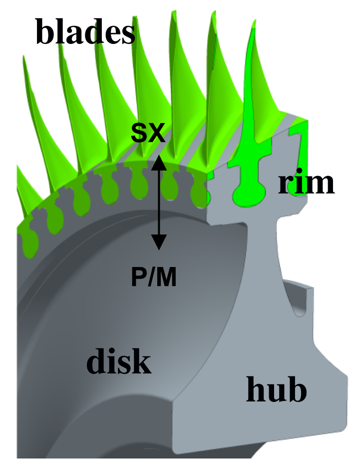

- **Model Ni-Based Superalloys**
  - Fundamental thermodynamic and kinetic underpinning of γ'-precipitation

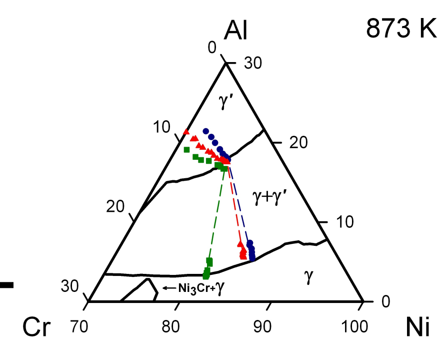

Atom-probe tomography measurements

APT: post-mortem atomic imaging technique in direct space with sub-nanometer spatial resolution (static snapshots of dynamic process)

1. Short-range ordering, clustering, impurity concentration & distribution
2. Morphological development
3. Dimensional and nanostructural quantification
   - Variations in layer thicknesses
   - Radius, number density, volume fraction of precipitates
4. Compositional characterization
   - Bulk phases
   - Fine scale nanostructure
   - Buried interfaces (e.g. grain boundaries):
     - Chemical interdiffusion, chemical roughness, segregation, transients

~50 million atoms

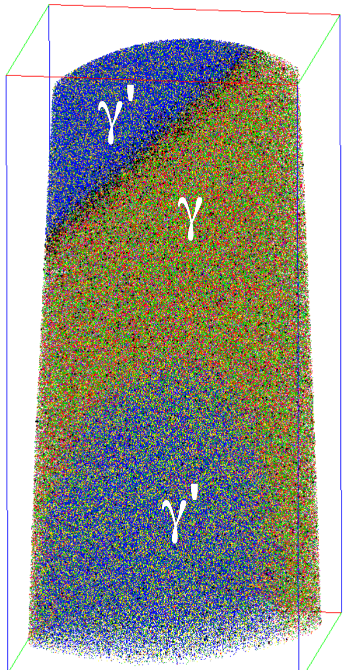

98 nm x 97 nm x 152 nm

3-D Atom Probe Tomography

Local Electrode Atom Probe (LEAP^{TM}) Imago Scientific 3000XSi

- **Analyze data with 3D visualization software, IVAS, from Cameca (formerly Imago Scientific)**

Determines the spatial position of individual atoms and their chemical identities with sub-nanometer scale resolution

Ion detection efficiency: 40-60%, Depth positioning: 0.02-0.05 nm, Lateral positioning: 0.2-0.3 nm

- ***Analyze volumes >10^6 nm^3***
  0.1 x 0.1 x 0.5 μm^3
- ***5 x 10^{-11} torr ultrahigh vacuum***
- ***Specimen T: 20 to 300 K***
- ***Equipped with both electrical and thermal-assisted pulsing:***
  - ***250 kHz electrical pulse***
  - ***500 kHz picosecond laser***
    (green: 532 nm, 10 ps)

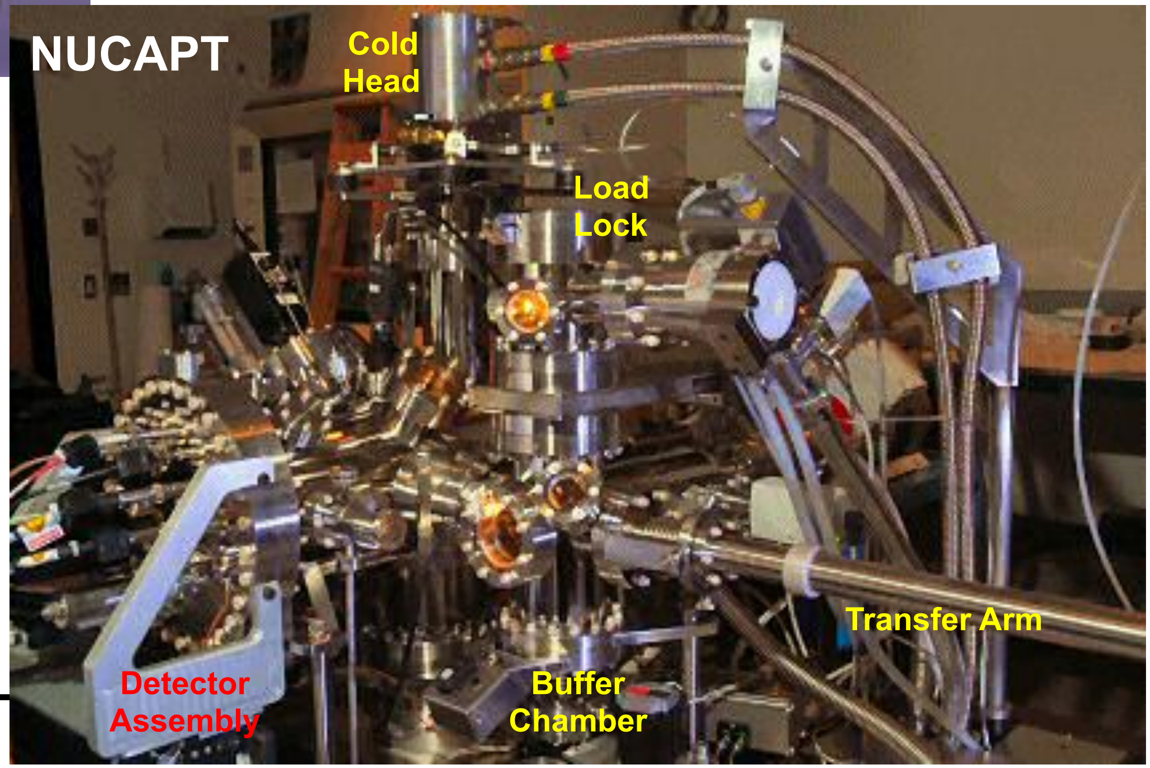

APT specimens are needle shaped

Metals: Electrochemical wire sharpening from APT blank (0.25 x 0.25 x 10 mm^3)

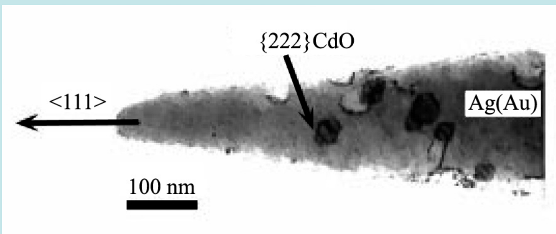

D. A. Shashkov, M. F. Chrisholm and D. N. Seidman
Acta. Mater, 47, 3939-3951 (1999).

Nanowires: Direct growth on a micropost

Silicon Micropost Array

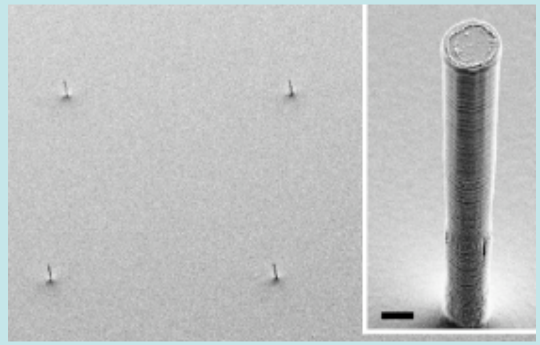

Perea et al. J. Solid State Chem, 181 (2008) 1642

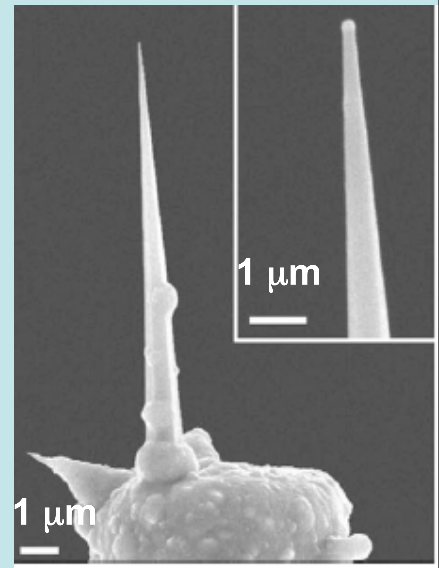

Multilayers: FIB preparation / Lift-out to micropost

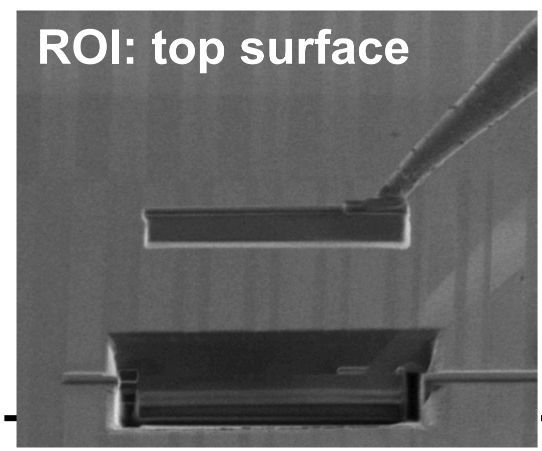

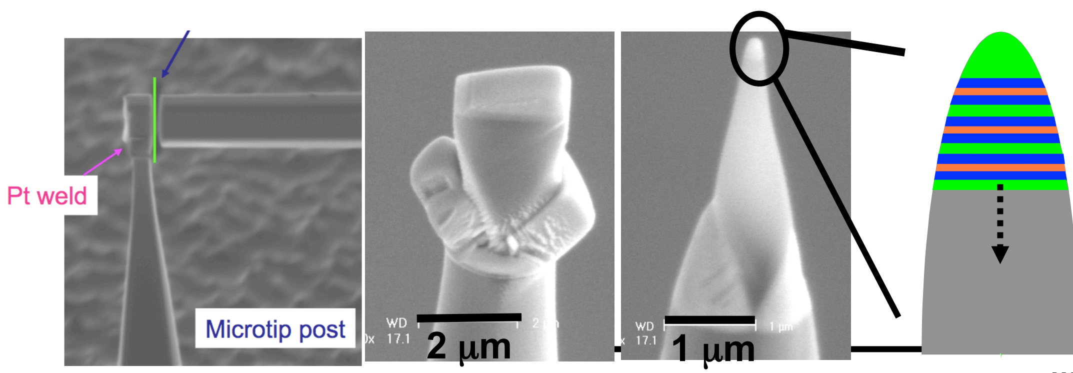

Tip radius is 50-100 nm

Pulsed-laser Atom Probe Tomography

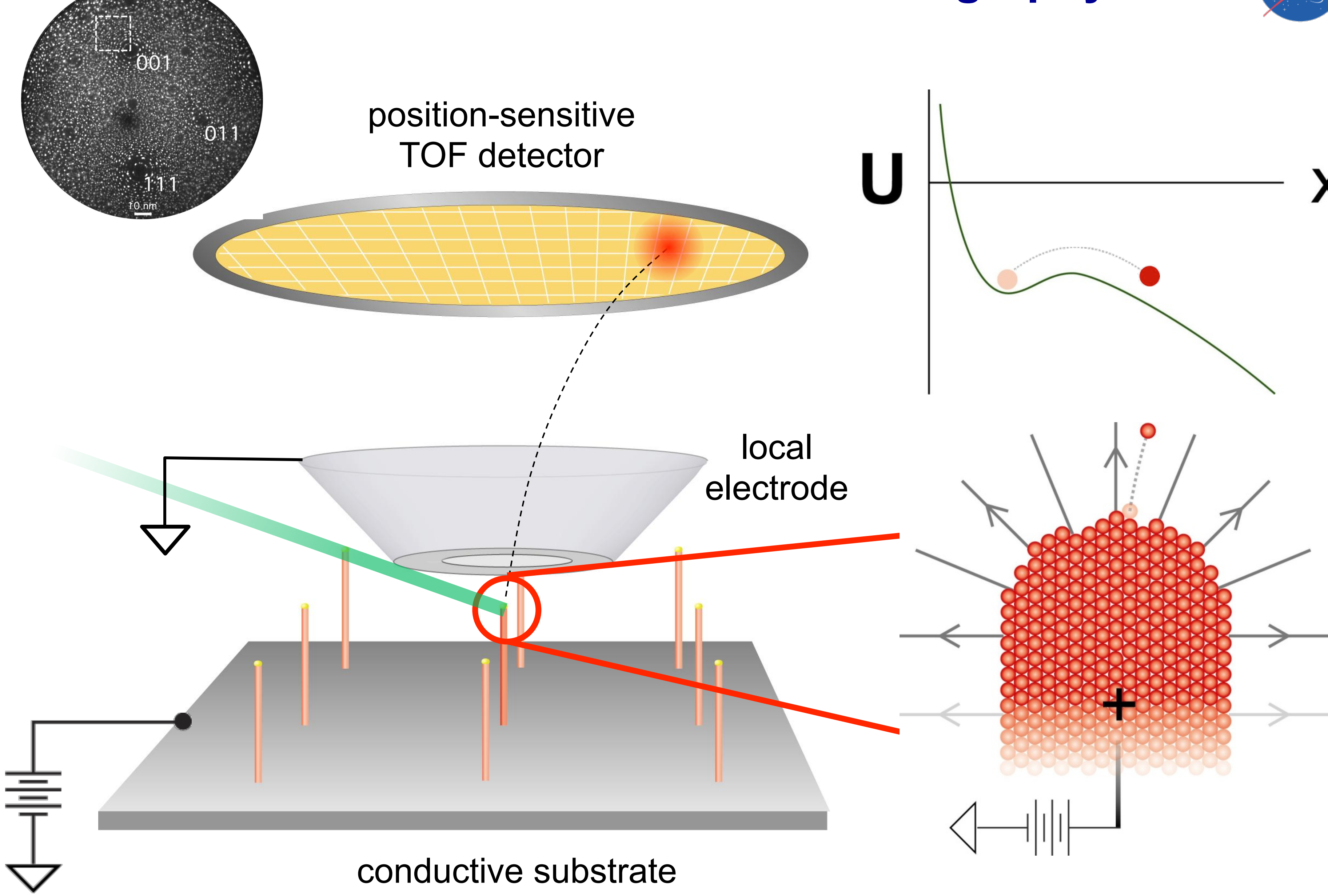

Courtesy of NUCAPT

National Aeronautics and Space Administration

Ions identified from their m/n signature (time-of-flight)

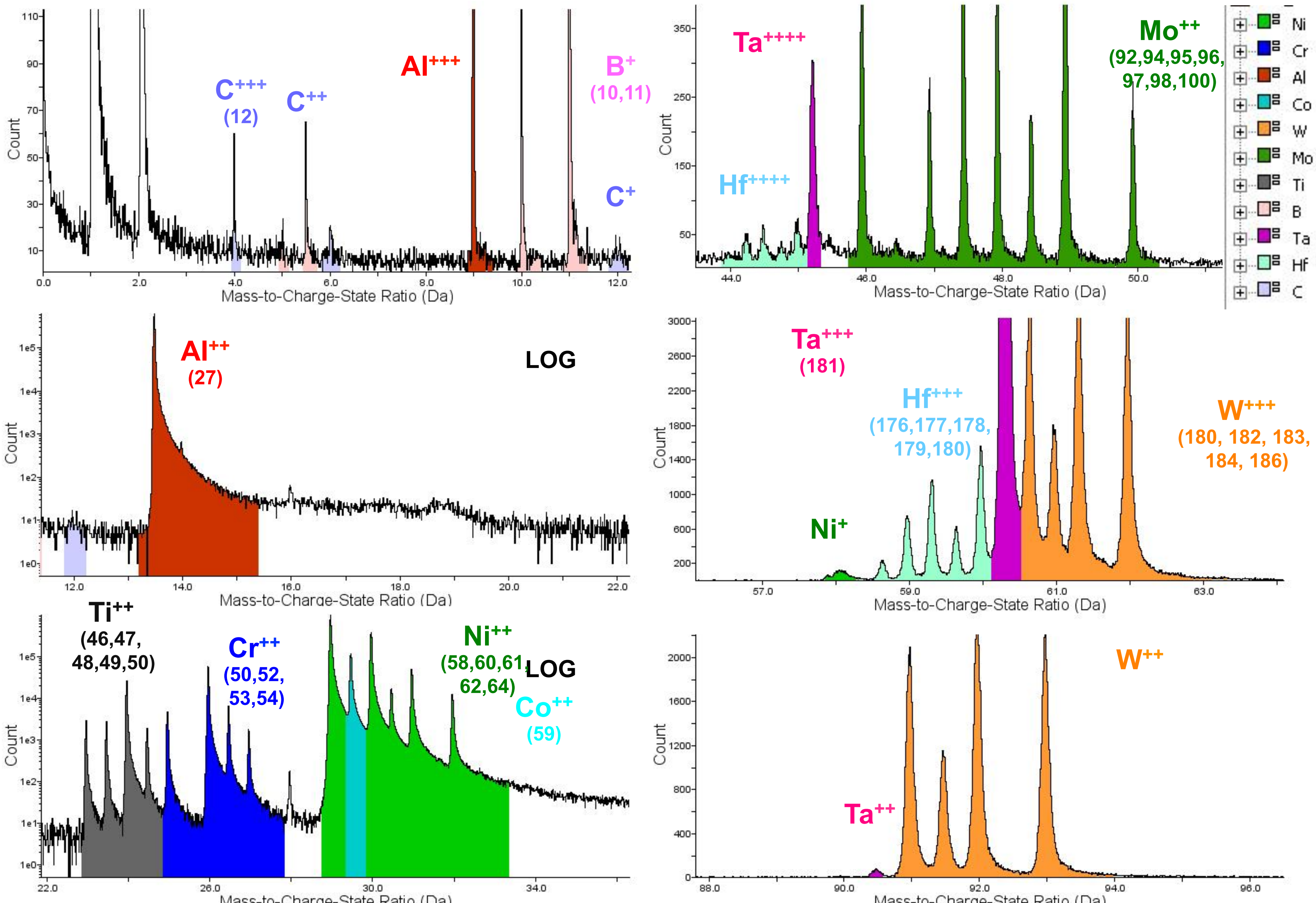

PL-APT Mass Spectrum for a Commercial Ni-based Superalloy

3-D LEAP™ Tomography

Specimens & Pucks

Specimen Carousel

Load Lock Chamber (Top Entry)

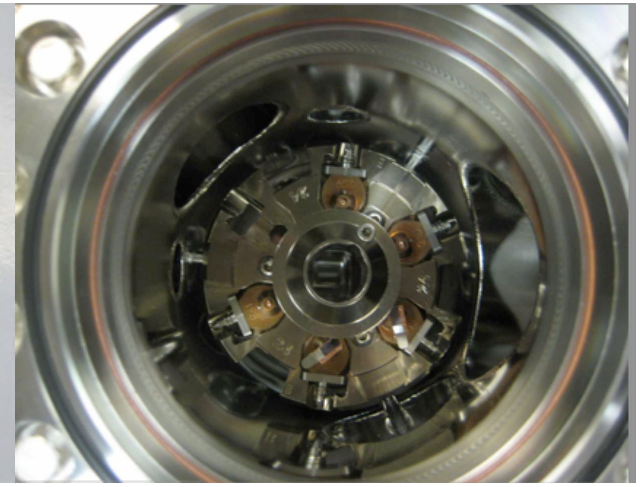

Analysis Chamber (Side Viewport)

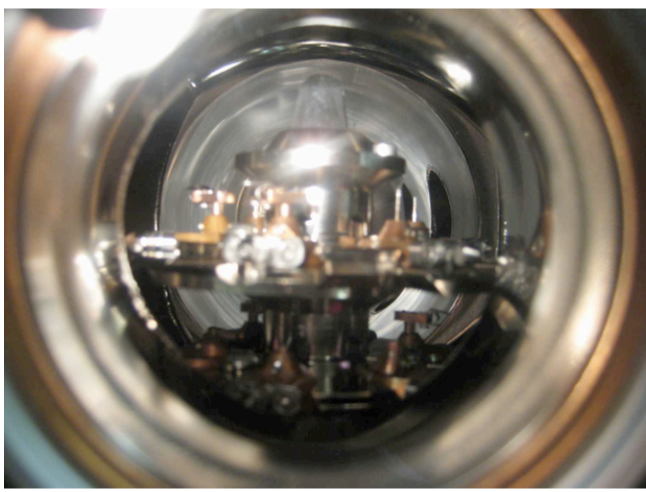

Courtesy of NUCAPT

Needle Geometry

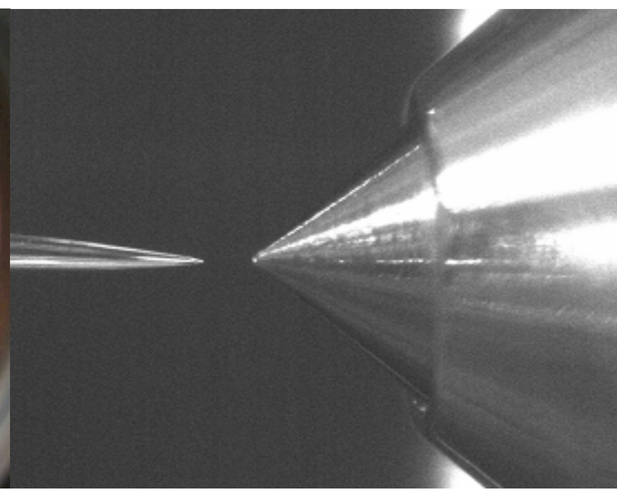

Microtip Geometry

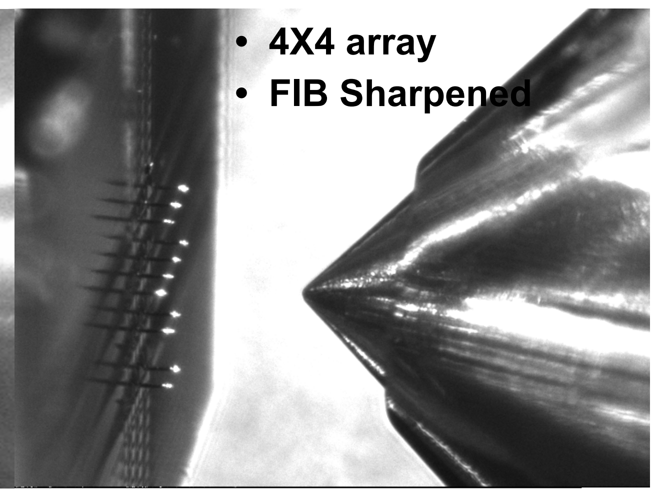

Courtesy of Imago

Fine scale microstructural analysis with APT

Ni-5.2 Al-14.2 Cr (at. %) aged at 600°C for 4 hours

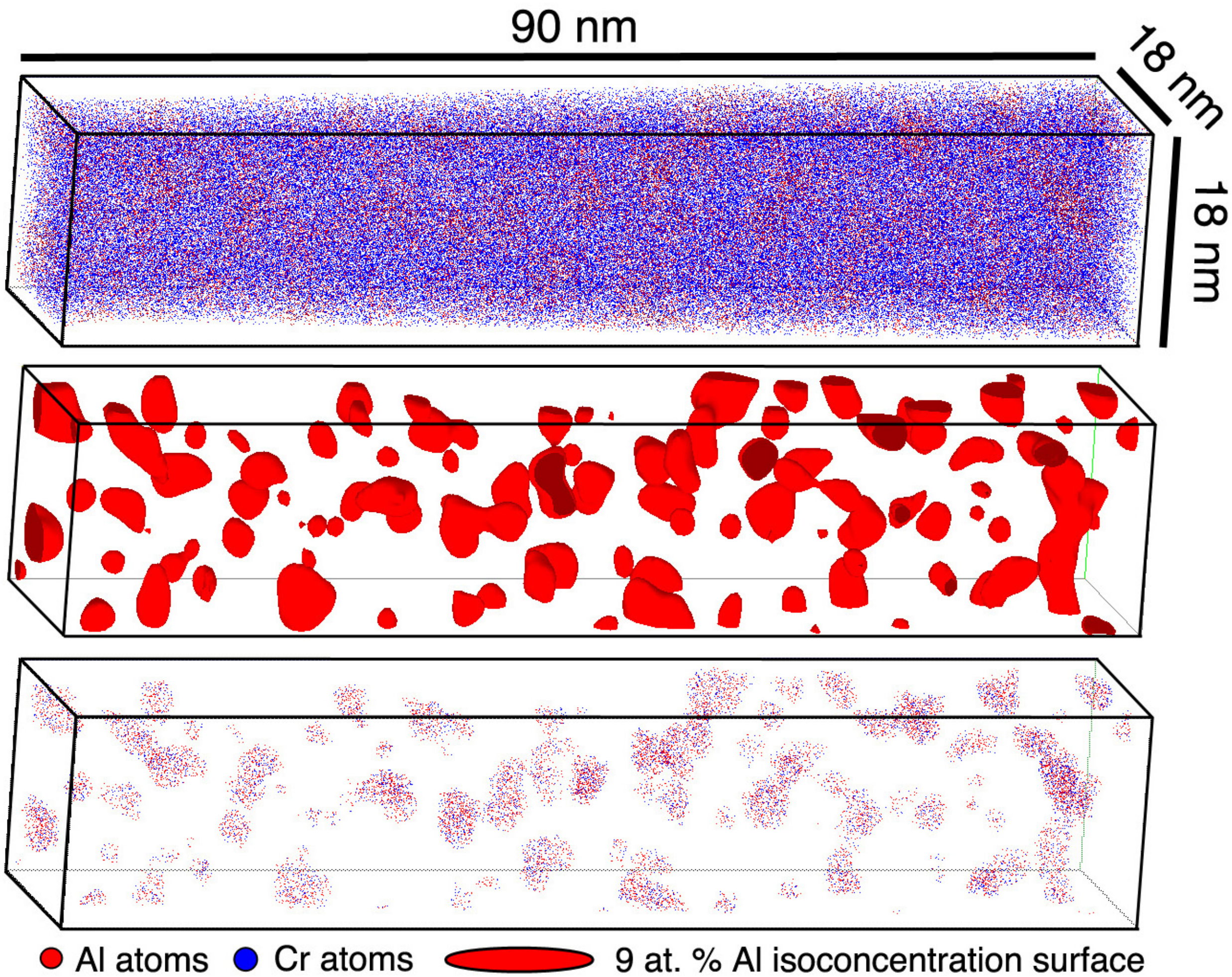

APT reconstructed volume

Isoconcentration surface

Selected volume

Proximity Histogram Concentration Profile

Data analysis in IVAS 3D visualization software

Proximity Histogram or "Proxigram" is a 3D nonlinear compositional profile with respect to isoconcentration surface (interfaces).

Three steps

1. **A sampling to generate a regular grid of concentration points**
2. **An interpolation to identify an isoconcentration surface**
3. **A correlation of the isoconcentration surface to the original set of discrete atomic positions**

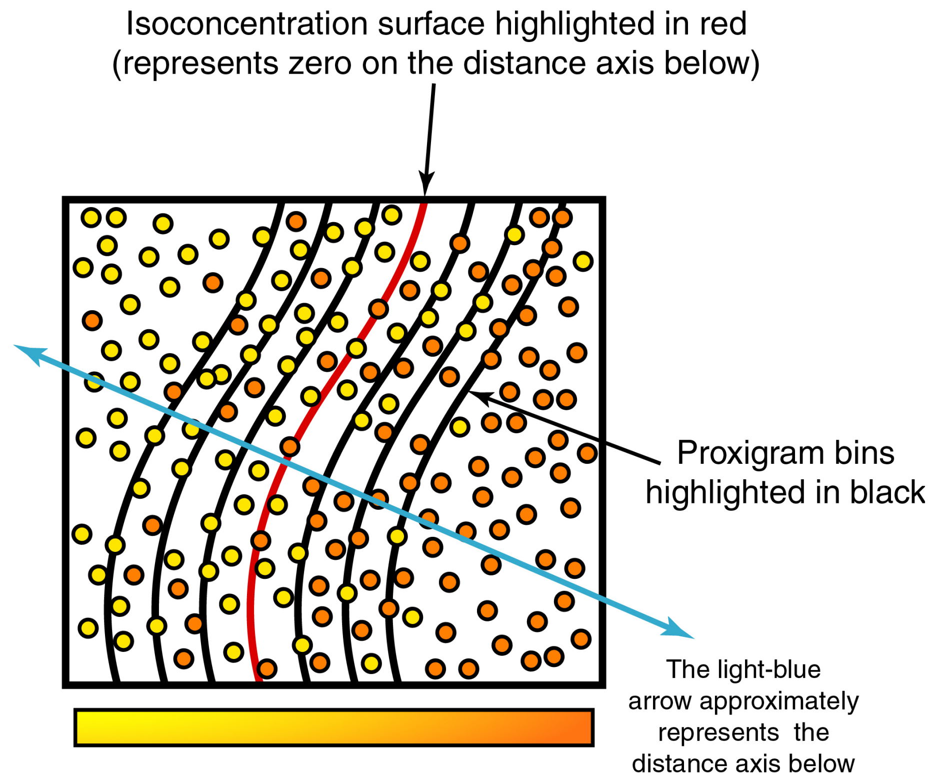

- Analyzes all the concentrations of the same value in a data set in parallel, invaluable for large data sets
- Invariant to interfacial geometry

Hellman, Seidman et al. *Micro. Microanal.* ***6****, 437 (2000)*

Decomposition behavior of model Ni-Al-Cr alloy when aged at 600 °C

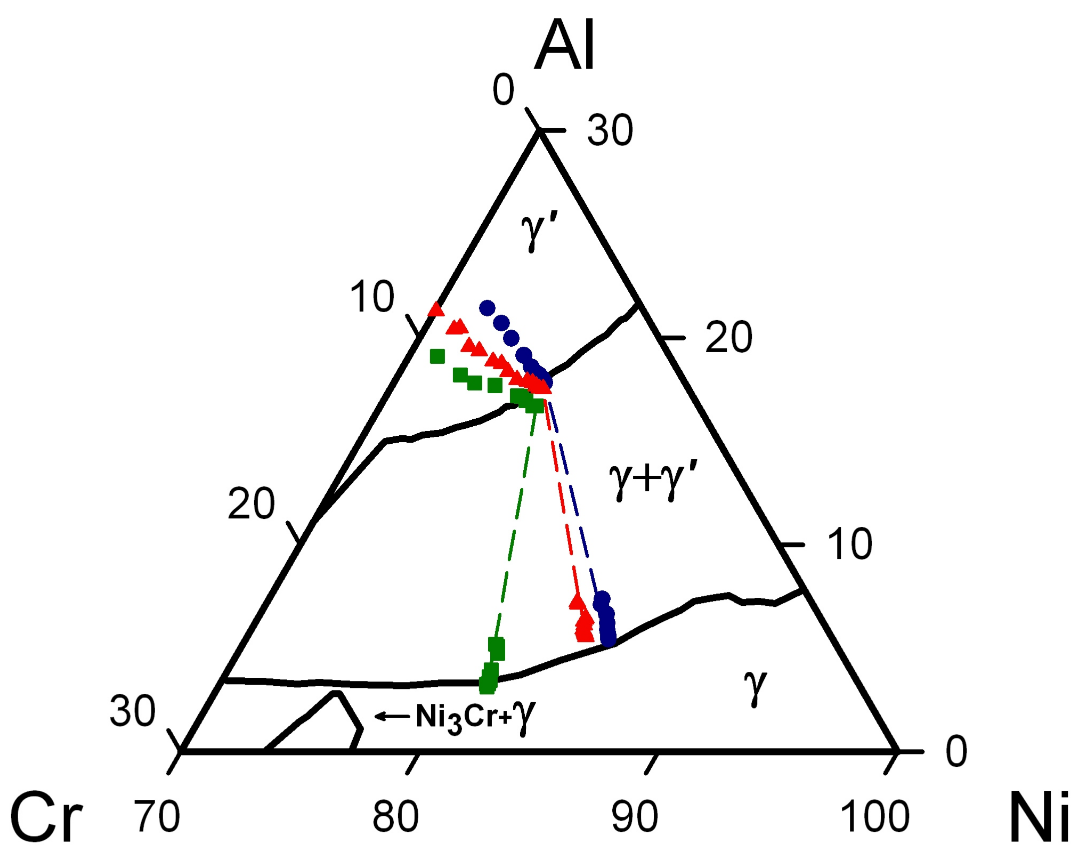

T= 600 °C aging studies of Ni-5.2 Al-14.2 Cr at. %

Atomic-scale mechanisms that drive the early stage precipitation

Moderate solute supersaturations, ϕ^{eq} = 15.6 %
(nondilute,nonideal)

$$\gamma\ (\text{fcc}) \xrightarrow[600°C]{T} \gamma\ (\text{fcc}) + \gamma'\ (L1_2)$$

Ni-Al-Cr → Ni-Al-Cr $Ni_3(Al_xCr_{1-x})$

1st-order ordering transformation

Increased aging

Short-range order and clustering → *Nucleation of γ' (mechanism)* → *Temporal evolution of the γ'-nuclei*

Nanostructural & Compositional Evolution

Atom Probe

Lattice Kinetic Monte Carlo

Clusters to precipitates radii up to ~10 nm

Seminal research of Schmuck *et al.* (Phil. Mag. A **76**, 1997, p.527) and Pareige *et al.* (Acta mat. **47**, 1999, p.1889)

Temporal evolution of γ'-precipitation in 3D

10 x 10 x 25 nm^3 sub-volumes of APT reconstructions

9 at. % Al isoconcentration surfaces (atoms omitted for clarity)

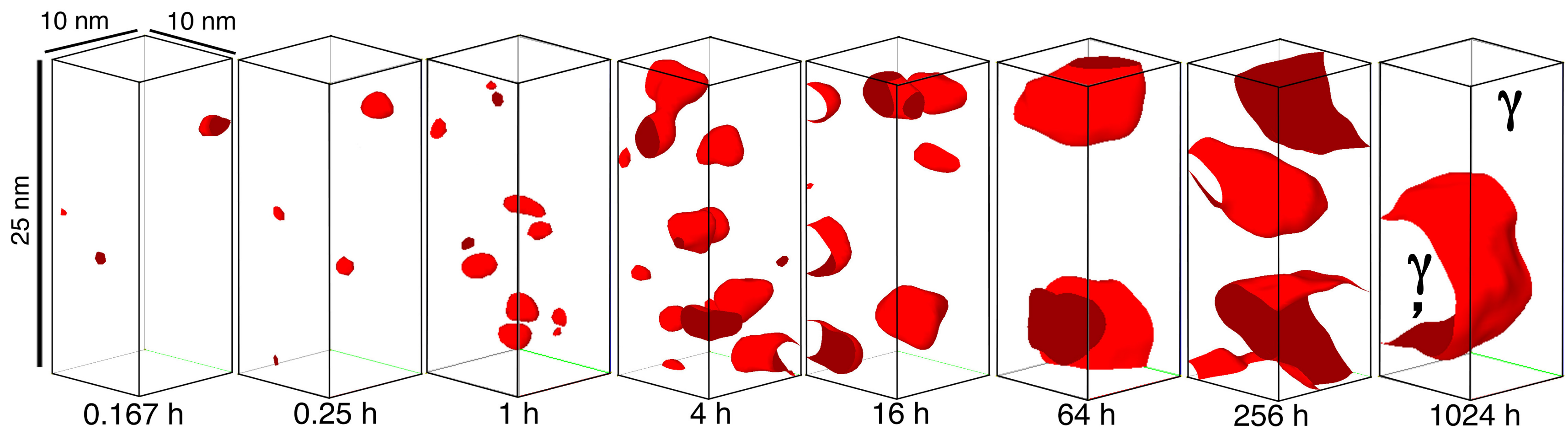

Ni-5.2 Al-14.2 Cr aged at 600°C

- **Precipitates as small as R = 0.45 nm are resolved, 20 detected atoms, which is close to lattice kinetic Monte Carlo (LKMC) predictions for critical nuclei size of 0.485 nm**
- **Dimensions and orientation of each precipitate are determined using best-fit ellipsoid**
- **Buried interfaces: generate average compositional profiles across the γ/γ' interfaces using proximity histogram compositional profiles**

Sudbrack et al, Acta Mater 54 (2006) 3199.

APT measurements of the mean precipitate radius

t (h)	Nb. of ppts. analyzed	$\langle R \rangle \pm \sigma$ (nm)
0.17	7.5	0.74 ± 0.24
0.25	74	0.75 ± 0.14
1	100	0.89 ± 0.14
4	173.5	1.27 ± 0.21
16	101	2.1 ± 0.4
64	46	2.8 ± 0.6
256	81	4.1 ± 0.8
1024	6	7.7 ± 3.3

nucleation

nucleation and growth

growth and coarsening

Sudbrack et al, Acta Mater 54 (2006) 3199.

Growth regimes established by APT measurements

Volume fraction of γ' (ϕ)

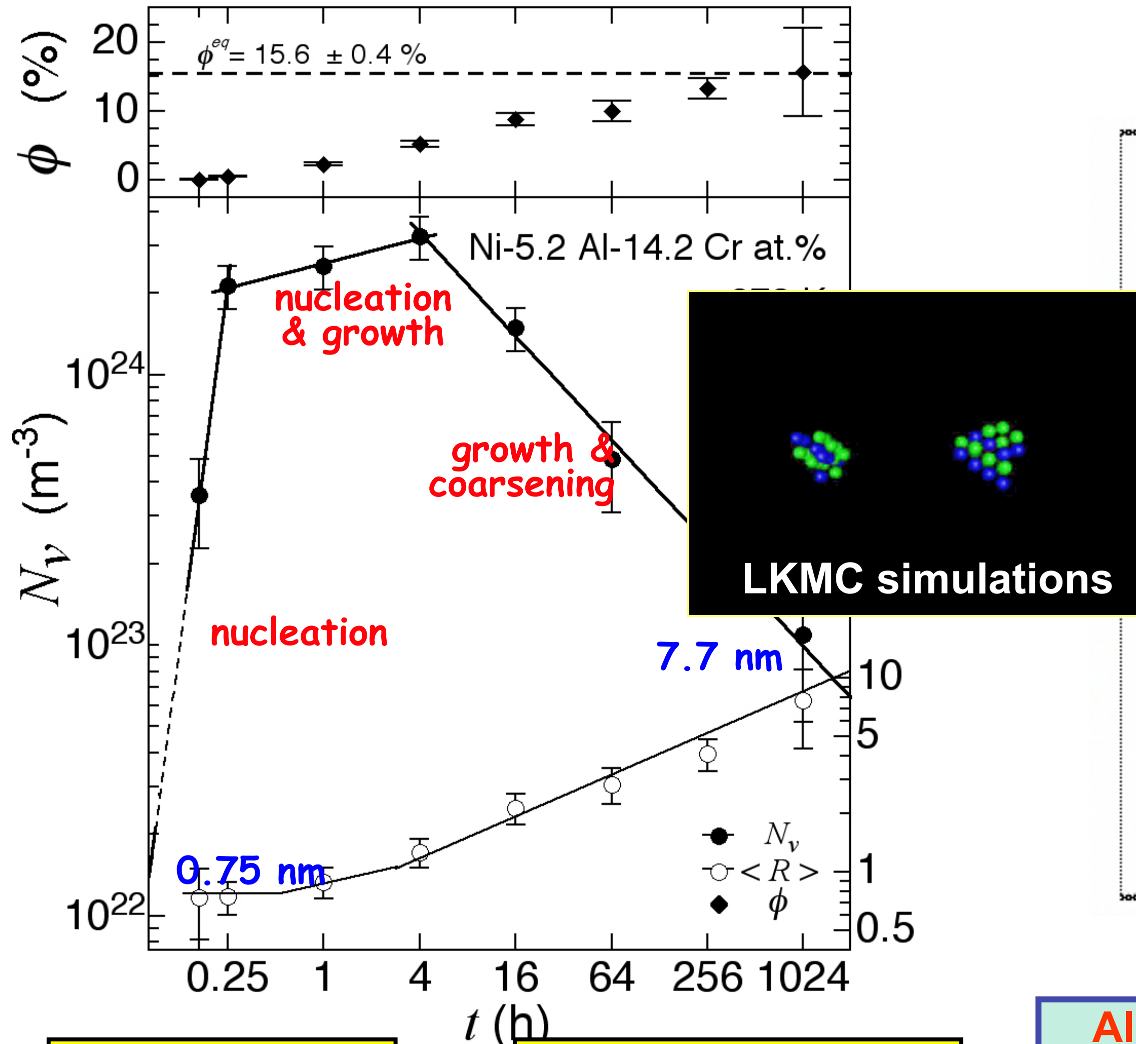

Example of γ' -precipitate pair connected by necked region

***t* = 4 h at peak N_v**

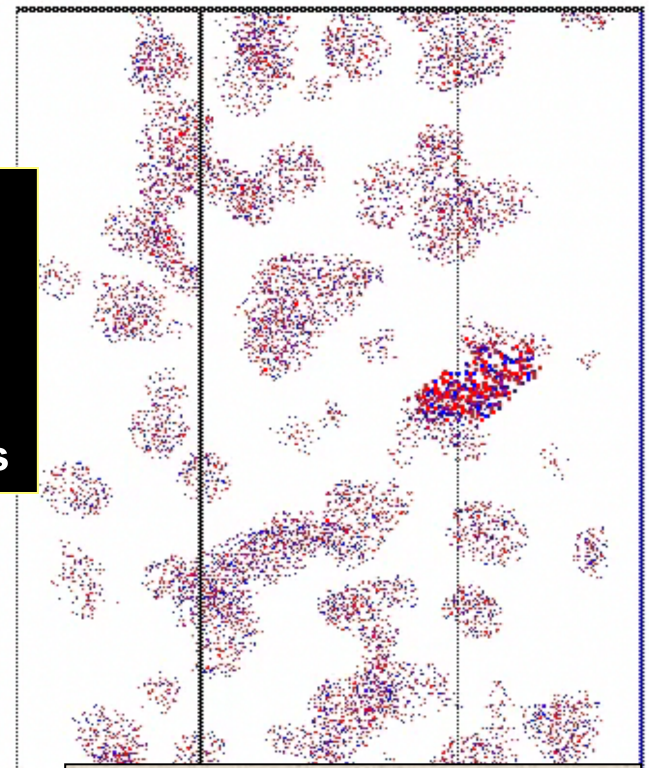

24 nm × 20 nm × 38 nm

Ppts. per unit volume (N_v)

Mean precipitate radius (<R>)

Al and Cr atoms within the 9 at. % Al isoconcentration surface displayed

Sudbrack et al, Acta Mater 54 (2006) 3199.

Concentration profile evolution in the matrix

Schematic: **Growth of stable nucleus** occurs by solute diffusion **driven by chemical potential gradient** due to supersaturated matrix

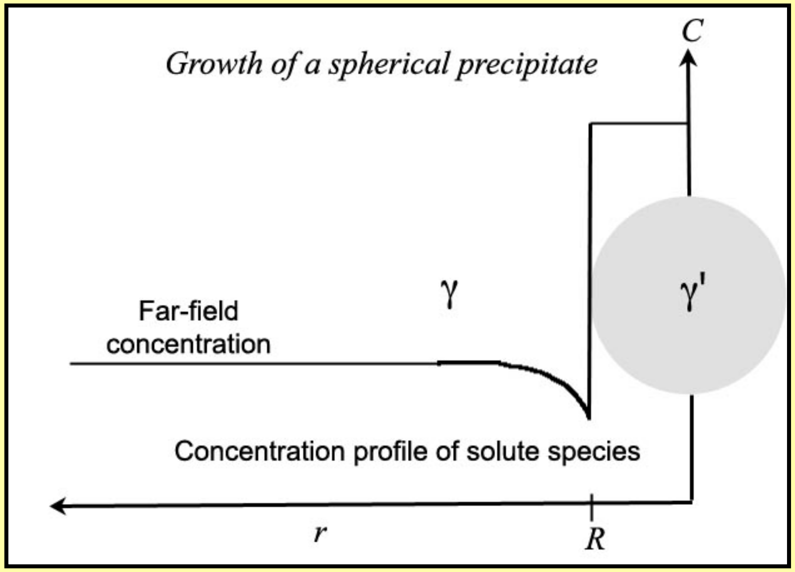

Transients disappear after 16 h
∴ quasi-steady state obtained

F. S. Ham, J. Phys. Chem. Solids, 6 (1958) 335

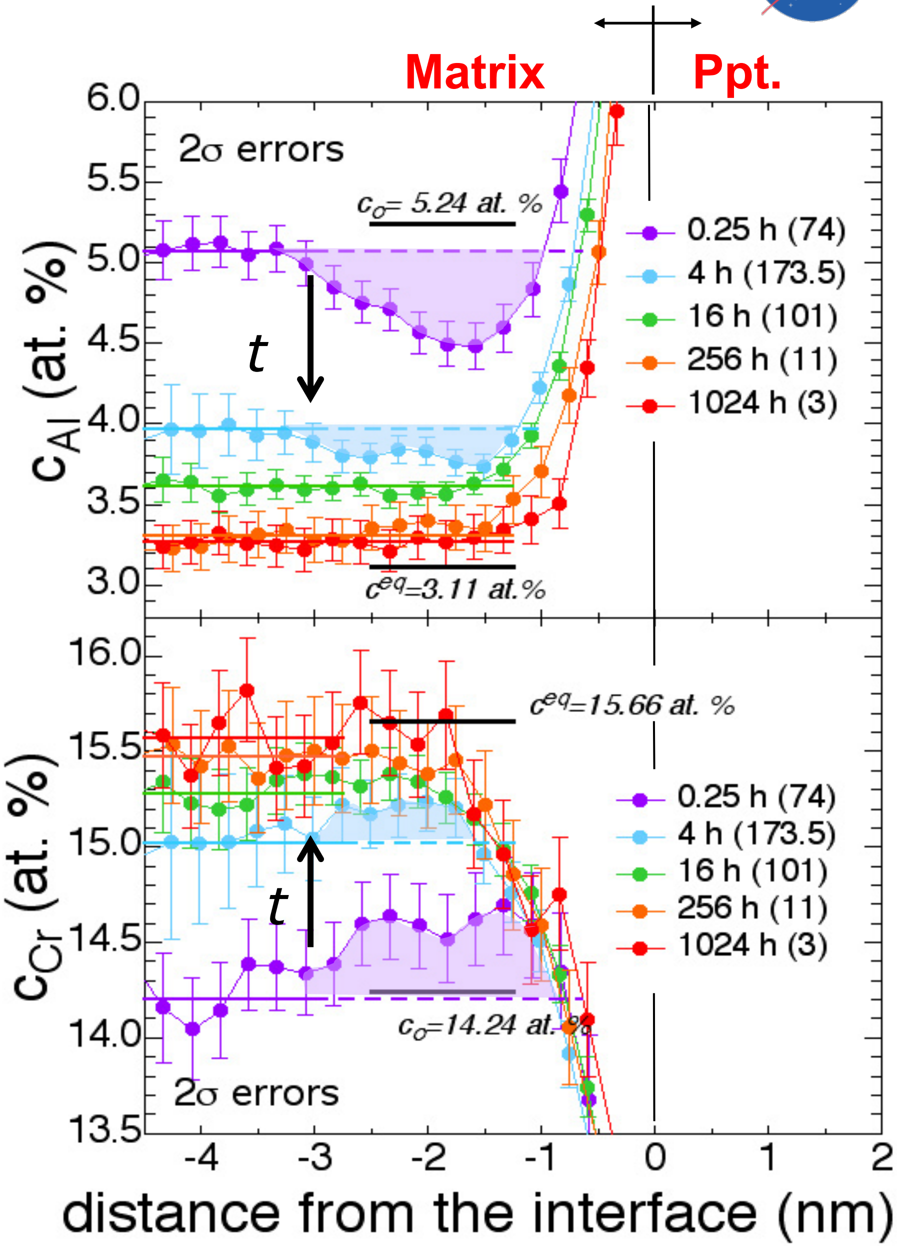

**** Proxigram method, which averages over all interfaces in the analysis volume***

Compositional evolution

Sudbrack et al, Acta Mater 54 (2006) 3199.

Matrix in the far-field

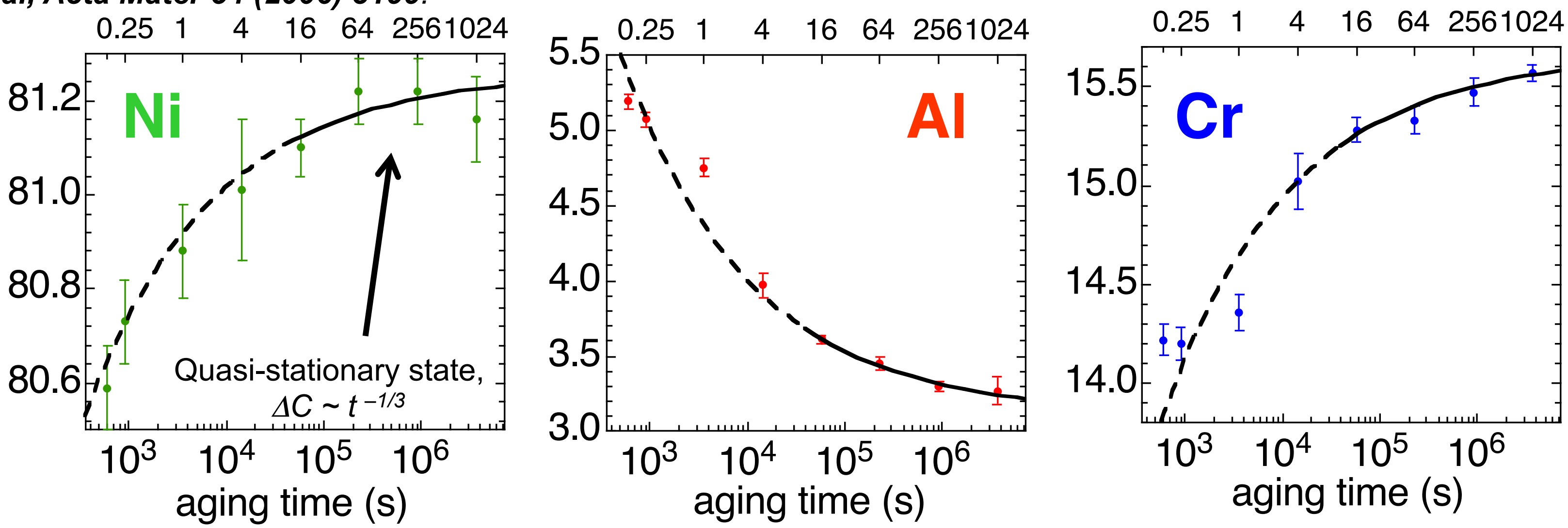

Precipitate Cores

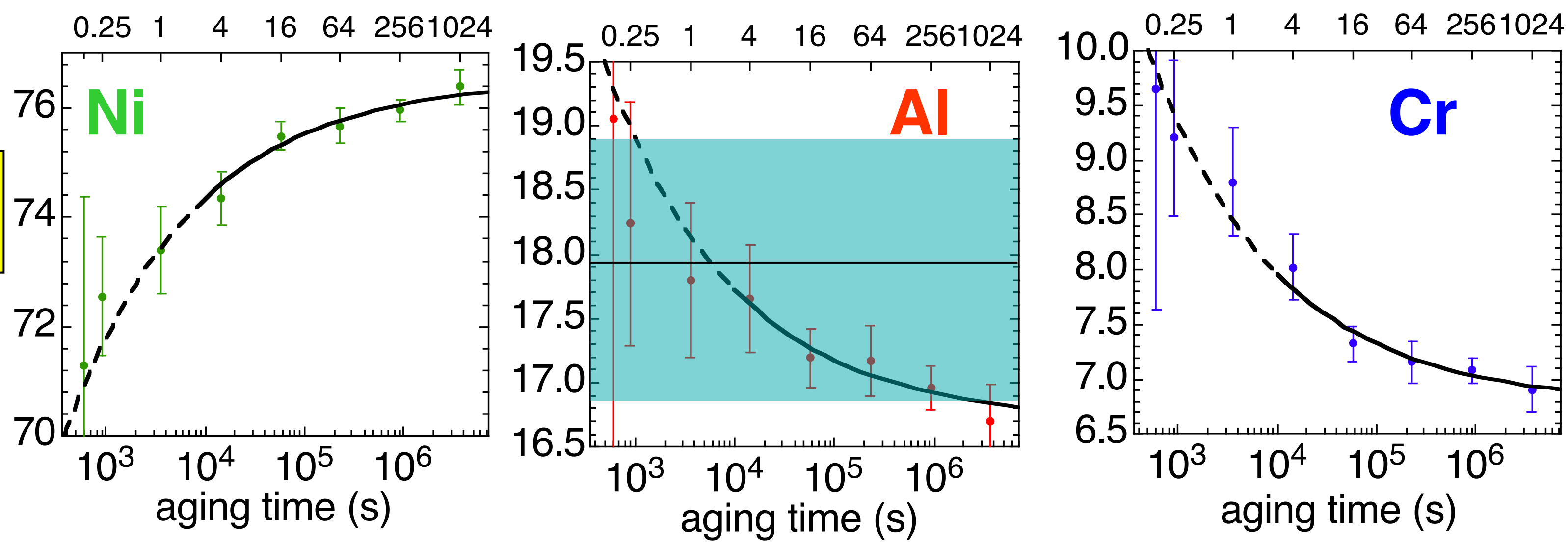

Gibbs-Thomson effect: predicts an increase in solid-solubility at an interface due its curvature. It is non-negligible when precipitate dimensions are on the of the order capillary length, typically 1-2 nm

See: Sudbrack et al, Acta Mater 55 (2007) 119.

Confirmation of early-stage coagulation & coalescence

LKMC simulations

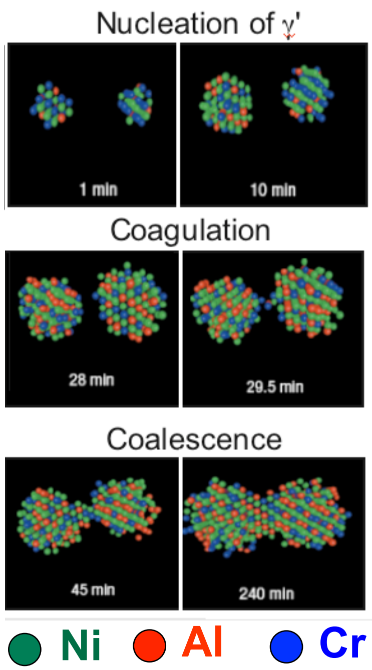

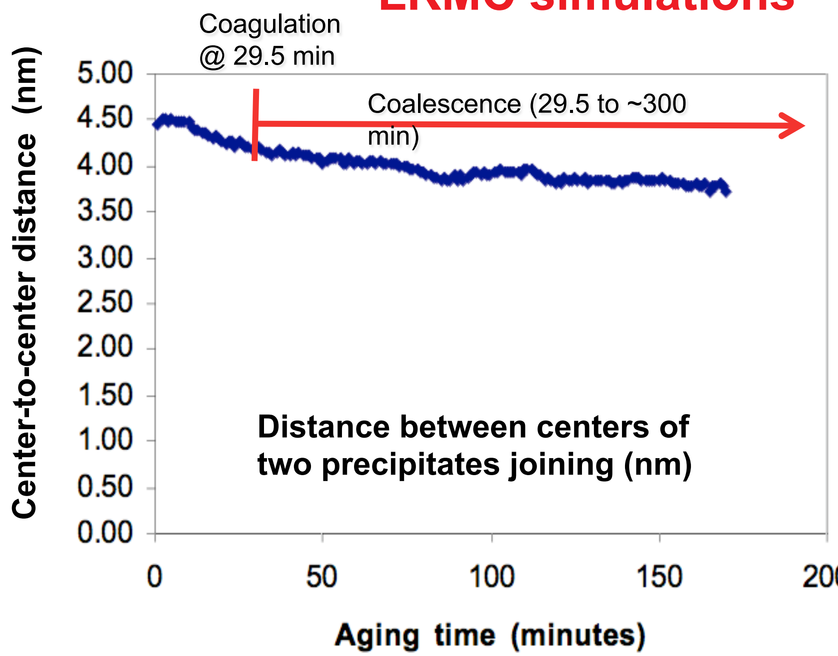

There are four $L1_2$ ordering variants

APB energy for two variants to join is 3-4 times larger than interfacial energy

--> Two precipitates must match variants to join

As much as 30% coalesced

Neck orientation distribution

pair

RA Karnesky, CK Sudbrack and DN Seidman, APL (2007).

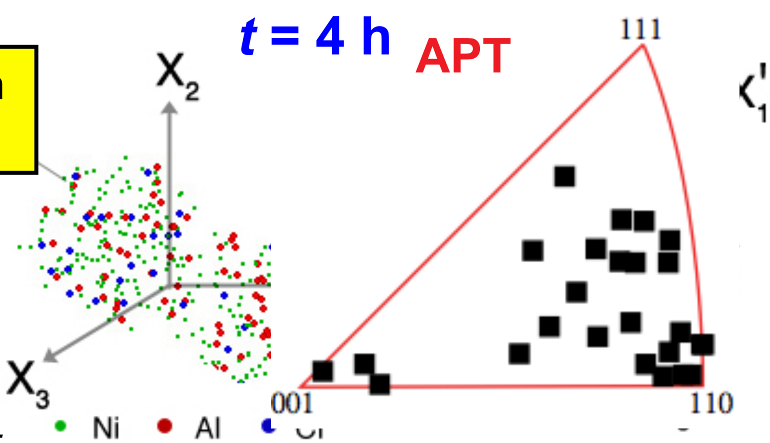

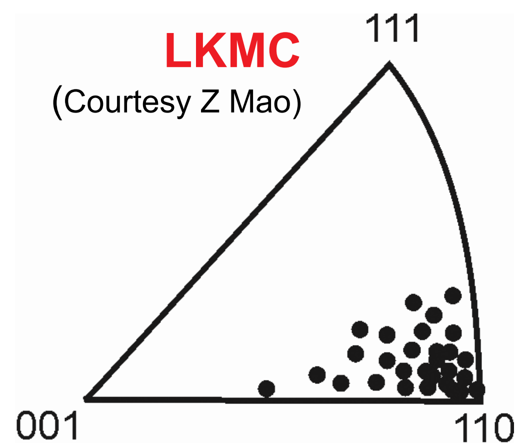

In FCC structure of the γ-matrix, <110> is fastest diffusion path for solute clusters

- **Atom probe tomography is a powerful characterization technique**

- **The combined APT/LKMC approach has been particularly helpful in:**
  - Nanometer scale characterization of morphological development in 3D
  - Precise compositional analysis of buried interfaces
  - Insight into diffusional processes that drive phase transformations